Raman Scattering and X-ray Diffraction of Ice in the Megabar Range. Occurrence of a Symmetric Disordered Solid above 62 GPa

Ph. Pruzan,* E. Wolanin, M. Gauthier, J. C. Chervin, and B. Canny

Physique des Milieux Condensés URA 782, Université P. et M. Curie, B77 F-75252 Paris, Cedex 05, France

D. Häusermann and M. Hanfland

ESRF, B. P. 220, F-38043 Grenoble Cedex, France

Received: October 11, 1996; In Final Form: April 25, 1997[⊗]

First results on a systematic study of ice by Raman scattering and X-ray diffraction in the megabar range are reported. Our discussion, which is based on the dynamical features of ice and its phase diagram, focuses on the possible occurrence of a symmetric state (ice X). It is concluded that above 62 GPa, delocalization of the proton occurs along O−O directions and ice may be symmetric from the statistical viewpoint.

1. Introduction

Investigation of ice at very high pressure is of importance in a number of fields such as solid state physics, physical chemistry, and planetary interiors. Lately a number of theoretical and experimental efforts were devoted to the understanding of that system below and beyond the megabar.[1−10] More than 20 years ago it was predicted that ice, in the 50−100 GPa range, transforms to ice X, the so-called symmetric ice or cuprite form of ice.[11] The existence of such a structure is yet to be proven.

The accurate knowledge of the physical properties of ice under pressure at variable temperature is required for the understanding of the evolution of this system under compression. With this aim we have undertaken, using Raman spectroscopy and X-ray diffraction, a systematic investigation of the two forms of ice, ice VII and ice VIII, which exist above ∼2 GPa. The spectroscopic data and the equation of state, derived from our X-ray analysis at ambient temperature, are discussed in connection with the occurrence of ice X. The most likely solid above 62 GPa is a symmetric proton-disordered solid which is a step toward ordered ice X.

2. Experimental Section

Diamond anvil cells (DAC) with incorporated pneumatic ram[12] were used for the experiments. The Raman setup was fully described elsewhere;[13] it permits investigation in the 10−300 K temperature range and, depending on the diamond anvil shape, up to 100 GPa or more. Full conical X-ray aperture (2 × 28°) DAC were used for X-ray diffraction. Investigations were performed at the European Synchrotron Radiation Facility on station ID9 using angle-dispersive powder diffraction and image-plate detector.[14]

3. Results

3.1. Raman Spectrum In the course of our Raman investigation, new data on ice VIII were obtained either (i) while determining the VII−VIII transition line or (ii) following four isotherms ranging from 50 to 200 K. We report here the data obtained during step (i). According to the pressure range, the VII−VIII transition line, plotted in Figure 1, was determined along isobaric or isothermal paths.[8] Ice VII is cubic (space group $Pn\bar{3}m$) with two molecules per unit cell on site symmetry

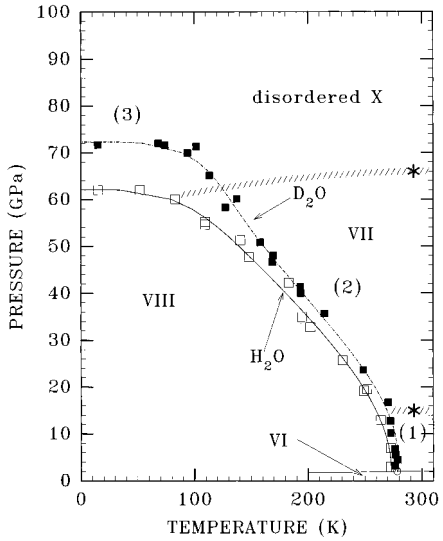

Figure 1. Ice VII−VIII transition line, pressure *p*(GPa) as function of temperature (K). Hollow and filled squares: experimental points for H_2O and D_2O, respectively. Solid and dotted lines: fit of the data for H_2O and D_2O, respectively. Hatched zones: expected transition lines from rotational disorder (1) to quasistatic disorder (2) and from quasistatic disorder (2) to translational disorder (3) named disordered ice X. This latter line is not shown for deuterated ice. ∗ : from X-ray data.

$\bar{4}3m$,[15,16] ice VIII is tetragonal (space group $I4_1/amd$) with 8 molecules per unit cell on site symmetry *mm*.[15] A marked modification of the *Raman lattice spectrum* characterizes the transition: In ice VIII two well-resolved translational modes were observed in the whole stability range, whereas in ice VII only a broad translational band was observed up to 40 and 50 GPa in H_2O and D_2O, respectively. Furthermore, as compared to ice VII, two librational modes were clearly observed in ice VIII up to 20 GPa in H_2O, in D_2O the lower frequency librational mode was followed up to 50 GPa.[8,16,17] It is to be noted that the lower frequency translational mode ($T_z(A_{1g})+T_{xy}(E_g)$) of ice VIII, which corresponds to the vibration between the two sublattices of ice,[18] softens above 50 and 60 GPa for H_2O and D_2O, respectively, that is on approaching the critical pressure where ice VIII vanishes at low temperature. The ν *vs* pressure curve of the upper frequency translational mode ($T_z(B_{1g})+T_{xy}(E_g)$) of ice VIII, which corresponds to the O−O stretching vibration of the body-centered cubic sublattices,

[⊗] Abstract published in *Advance ACS Abstracts,* June 15, 1997.

S1089-5647(96)03182-3 CCC: $14.00

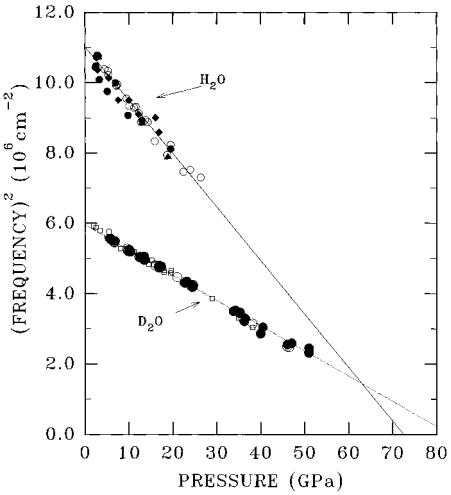

Figure 2. Square of the phonon frequency $\nu_1(A_{1g})$ (10^6 cm^{-2}) in ice VII and VIII for H_2O and D_2O, respectively, as function of pressure. Experimental points: H_2O (○) ice VII and (♦▲●) ice VIII; D_2O (□○) ice VII and (●) ice VIII. Solid and dotted lines are fits according to eq 1.

and the one of the translational band found in ice VII superimpose. At low pressure the isotopic ratios of the lattice modes are close to the values given by Wong and Whalley;[18] we found in order of increasing frequency 1.03 and 1.07 for the translational modes and 1.28 and 1.34 for the librational modes. The pressure dependence of these ratios are concave downward curves with maxima around 18 GPa for translational modes and 14 GPa for librational modes.

In ice VII, the stronger intensity *vibron mode* $\nu_1(A_{1g})$ (the symmetric OH stretching vibration), hereafter called ν_{OH}, was followed up to 50 GPa in D_2O and, due to the diamond two-phonon absorption, to 25 GPa in H_2O. In ice VIII data were obtained up to 50 GPa; they superimpose on the ice VII ν_{OH} data. The vibron frequency decreases with pressure with an average slope $d\nu_{OH}/dp$ around -20 cm^{-1}/GPa; its pressure dependence is not linear. Above 10 GPa it is concave downward. It was observed, as shown in Figure 2, that plots $\nu^2_{OH(OD)}$ *vs* pressure are straight lines.[19] This pressure dependence which may be expressed as

$$\nu_{OH(OD)} = (\nu_o^2 - ap)^{1/2} \qquad (1)$$

where ν_0 and a are parameters, suggests a soft-mode behavior.[20,21] The vibron isotopic ratio is found close to 1.36 at 2 GPa; it decreases to 1.32 at 25 GPa. Its variation *vs* the oxygen−oxygen distance d_{OO} is compared to that of O−H···O systems at ambient in Figure 3. This comparison is discussed in the next section. Based on the correlations obtained in hydrogen bonded systems at ambient pressure, negative shift of the vibron frequency ν_{OH} and drop of its Raman intensity were major arguments concerning the lengthening of the covalent bond as pressure increases. However, from the quantitative viewpoint the respective behaviors of ambient systems and of ice under pressure are different (see ref 19 and next section).

3.2. X-ray Diffraction. Details about this work are given in ref 14. Several sets of data were collected in ice VII at 293 K, specifically, the 110, 200, and 211 reflections were followed up to the maximum pressure of 106 GPa. Corrections from the effect of uniaxial stress component were performed. The 51 volume data points, obtained in the 3−106 GPa pressure range, exhibit a regular variation. However, correlated with slope changes of the VII−VIII transition line, regime changes

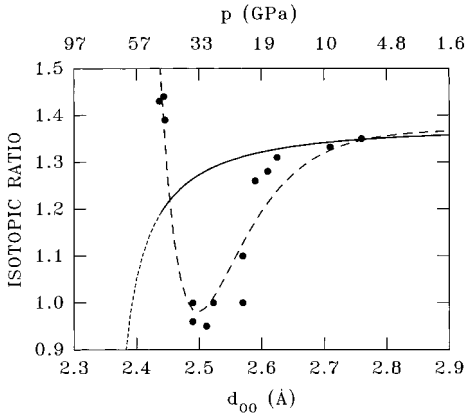

Figure 3. Isotopic ratio ν_{OH}/ν_{OD} as function of d_{OO} (Å) (top: pressure p(GPa)). Filled symbols: systems at ambient pressure (from ref 25). Broken line: fit for systems at ambient pressure. Solid line: isotopic ratio of ice up to ∼50 GPa according to eqs 1 and 2. Broken line: extrapolation.

of the proton disorder are expected at ∼15 and ∼60 GPa [8,19,22] (see also next section) which should cause higher order transitions. For the search of these weak effects, we used a linear form of the equation of state (EOS) of solids which may be obtained through the analytical form proposed by Vinet *et al.*[23] which reads

$$p = 3\frac{B_0(1-x)}{x^2}\exp\left[\frac{3}{2}(B_0' - 1)(1-x)\right] \qquad (2)$$

with $x = (V/V_0)^{1/3}$ where V and V_0 are the molar volume at the pressure p and at ambient, B_0 and B_0' are the bulk modulus and its pressure derivative. In absence of transition, eq 2, in the system of coordinates $\ln[p(x^2/3(1-x))]$ *vs* $(1-x)$ is linear. Actually, such a plot of our data exhibits three linear domains, with changes occurring at 15 and 66 GPa (*i.e.*, very close to the expected transition pressures). As shown by the smooth variation of our volume data points, these effects are weak, and eq 2, with $B_0 = 14.9$ GPa, $B_0' = 6.3$ and $V_0 = 12.087$ cm^3 mole^{-1}, may be used to fit our data with sufficient accuracy. This equation, which is quantitatively close to that of Hemley *et al.*,[24] was used in the following for the computation of the d_{OO} distance under pressure.

4. Discussion and Conclusion

The correlations ν_{OH} *vs* d_{OO} and d_{OH} *vs* d_{OO}, where d_{OH} is the covalent bond length, established at ambient pressure from O−H···O systems, have long been considered to be valid for ice under pressure. Recent results[3−5,19] have demonstrated that the above comparisons are not correct from the quantitative standpoint. In short, as compared to systems at ambient pressure, the ν_{OH} and d_{OH} variations *vs* d_{OO} for ice under pressure are shifted to the left as if symmetrization occurred for lower d_{OO}.[19] This conclusion may be illustrated by the following observations: (i) For symmetric systems at ambient pressure, d_{OO} is found close to 2.44 Å with $\nu_{OH(OD)}$ around 800 and 500 cm^{-1} for protonated and deuterated systems, respectively.[25,26] In ice and deuterated ice under pressure this frequency value should be obtained at 67 and 79 GPa, respectively (eq 1), that is, for $d_{OO} = 2.37$ and 2.34 Å (eq 2).

(ii) If the lengthening of d_{OH} with decreasing d_{OO}, for systems at ambient pressure, is observed from $d_{OO} = 2.9$ Å, it is not the case for ice under pressure, where neutron diffraction in D_2O indicates an approximate constant value for d_{OD} up to 25 GPa, the upper pressure investigated.[3−5] From the discussion of the

VII−VIII transition curve it was shown that d_{OH} is expected to increase from $d_{OO} \sim 2.5$ Å (*i.e.* for pressures above 40 GPa).[19]

(iii) The isotopic ratio ν_{OH}/ν_{OD} of ice, plotted in Figure 3, drops for shorter d_{OO} distances than in systems at ambient. Equation 1, which is used with eq 2 to compute this ratio, is expected to hold up to ∼50 GPa (where $d_{OO} = 2.42$ Å) (*i.e.*, in the pressure range where it was possible to observe the vibron in D_2O). For systems at ambient pressure, the isotopic ratio decreases from 1.35 to 0.95 for d_{OO} varying from 2.9 to 2.5 Å. Compounds for which the lower isotopic ratio of ∼0.95 is observed correspond to a proton double-well potential with a delocalization of the proton while the deuterated systems are ordered.[25] For $d_{OO} \sim 2.44$ Å the isotopic ratio increases to ∼1.4. This limit corresponds to a symmetric bond with a single central minimum either for protonated or deuterated compounds.[25] In fact it was pointed out that the proton potential varies continuously from double to single minimum with decreasing d_{OO} distances from 2.5 to 2.44 Å.[27] The above picture agrees well with what is expected in ice above 60 GPa from the shape of the VII−VIII transition line (see the following and refs 8 and 19). In ice, an isotopic ratio around 0.95 is expected at ∼64 GPa (Figure 3 and eqs 1 and 2) that is for $d_{OO} = 2.38$ Å. In this pressure range, a proton delocalization is expected in ice but not in deuterated ice. Delocalization in deuterated ice occurs around 72 GPa. Assuming now that the dependence of the isotopic ratio of ice *vs* d_{OO} is similar to the one of ambient pressure systems but with a minimum located at 2.38 Å, the single-well potential symmetric state may be reached for d_{OO} around 2.32 Å that is for pressure around 90 GPa.

An important feature, mentioned above, is the dynamics of the system: In a proton delocalized system, the proton site may be statistically at the center of the O···O distance, but if symmetric ice refers to the cuprite Cu_2O structure, it corresponds to a single-well potential for the proton whose site is therefore localized. In most of the recent papers this point has been forgotten, though it was discussed for systems at ambient pressure;[25−27] moreover, a description of ice under pressure in terms of proton density, based on the double-well potential model, was given by Schweizer and Stillinger.[28] This point is commented at the end of this section.

As mentioned in section 3.2, higher order transitions are expected in ice VII around 15 and 60 GPa; this is suggested by the VII−VIII transition line shape and its analysis with the pseudospin formalism.[8,19,22] Some main features are worth recalling in view of the phase diagram proposed here.

From 2 GPa up to pressures exceeding 62 and 72 GPa for ice and deuterated ice VII, three regimes are expected for the proton disorder: (i) Around 2.5 GPa, ice VII is orientationally disordered.[15] Due to the increase of the intermolecular forces, the rotational tunneling is expected to decrease rapidly with pressure as observed for instance in methane.[29] Actually a change of slope of the transition temperature T_c *vs* pressure curve, is observed around 12−18 GPa. In this pressure range, the width of the vibron ν_{OH} exhibits a marked minimum[16] and the linear form of our EOS shows a change of slope (section 3.2).

(ii) Above ∼15 GPa a regular decrease of T_c with pressure, similar to what is encountered in other H-bonded compounds, is observed. The physical model generally used to account for this behavior is the pseudospin formalism (see ref 21 and references cited therein). Briefly a symmetric proton double-well potential is assumed; the O−H···O units interact through a dipolar interaction J which is a factor of order, while the proton-tunneling value Ω, which causes dipole moment inversion, favors the disorder. The decrease of T_c with p can be understood in terms of an increase in tunneling frequency and/or a decrease in the dipolar interaction until a critical ratio Ω/J is reached. Our previous analysis of the VII−VIII transition line[8,19] showed that from ∼16 to 50 GPa (from 16 to 70 GPa for D_2O) the tunneling effect does not play any role in the determination of the transition temperature which is given by the Ising model:

$$T_c = \frac{J}{4k_B} \tag{3}$$

At T_c the long-range dipolar order, found in ice VIII, disappears; in ice VII, due to the ice rule, a short-range order exists and may concern a few crystallographic cells.[16] A reordering of these small clusters may occur because the tunneling frequency is not negligeable. On the other hand, in ice VIII, the order prevents the proton tunneling because it should be a collective effect; the long-range order may cause an asymmetry of the double-well proton potential. The model involved in eq 3 is indirectly supported by neutron diffraction results. The intersite separation δ of the proton double-well may be computed from eq 3. It was found that, in the ∼16−44 GPa range (the pseudospin formalism does not hold in the region of orientational disordering), the pressure dependence of δ is similar to that of d_{OO}; in other words, d_{OH} is constant in this range.[19] The neutron diffraction data confirm this trend.[3−5] This result is also found from *ab initio* computations.[2−4]

(iii) A limit of stability in pressure for ice VIII is reached around 62 and 72 GPa for H_2O and D_2O (*i.e.*, in the plateau region where T_c drops to 0 K). This effect is accounted for the increase of Ω, or more accurately, of Ω/*J*, which reaches a critical value.[8,19] Actually it is likely that in this pressure range the proton disordering is due to the delocalization of the proton site: the zero-point energy being equivalent to the potential-barrier height. The extrapolation of the *ab initio* computation of B. Silvi,[4] and the abrupt change of slope of the D_2O transition line support that viewpoint. The H_2O transition line shows a smoother variation above 50 GPa suggesting that tunneling effect may play a role below the critical pressure.

We conclude that from both sides of the plateau the proton potential is a double-well type. Above the critical pressure (62 or 72 GPa) the proton site is delocalized or more precisely translationally disordered. As mentioned above this description fits with the conclusions obtained from the isotopic ratio variation *vs* d_{OO} distance. The approach of the plateau from below causes a progressive proton disordering: this is indicated by the strong broadening of the stretching lines observed in Raman scattering and infrared absorption.[8,9,16] However, the transition to a symmetric disordered system occurs in a relatively narrow pressure range as shown either from the experimental features of the transition line and the slight softening, observed over 10 GPa, of the vibration $T_z(A_{1g})+T_{xy}(E_g)$ involving the two sublattices of ice VIII.[8,19]

The pressure of stability limit, where the proton delocalization occurs, depends on both the pressure dependences of the potential barrier height and of the vibron frequency, accordingly it depends weakly on temperature. This critical pressure whose location extends above 100 K (*i.e.*, above the stability domain of ice VII) must be a flat curve in the *p,T* diagram. Till now the only confirmation was obtained from our EOS, the transition location at 293 K being close to 66 GPa. Consequently the hypothetical line between ice VII, which involves localized proton sites and the solid with delocalized proton sites, is drawn in Figure 1 for H_2O between 62 GPa (80 K) and 66 GPa (293

K). In the same way, the line between the rotational disorder and the quasistatic disorder at ∼15 GPa is plotted in Figure 1.

On further compression, the double well is expected to transform into a single well. From the isotopic ratio the pressure where this transformation is achieved is estimated around 90 GPa, which is likely a lower limit. This transformation is very likely a continuous process; consequently the location of the ordered solid will be difficult to determine accurately. This progressive ordering is consistent with the narrowing of the various bands observed with infrared spectroscopy on compression above 60 GPa.[9]

In the solid above 62 GPa (*i.e.*, above the plateau and its extrapolation at higher temperature) it is concluded that the proton site is disordered between two oxygens and may be statistically at the midpoint. However a more accurate picture, when delocalization occurs, is given by the proton density function. As shown by Schweizer and Stillinger,[28] the transition to ice X would involve a stepwise sequence through a solid rather close to ice VII with a strong dynamic disorder along O···O directions.

References and Notes

(1) Lee, C.; Vanderbilt, D.; Laasonen, K.; Car, R; Parrinello, M. *Phys. Rev. B* **1993**, *47*, 4863.

(2) Ojamaë, L.; Hermansson, K.; Dovesi, R.; Roetti, C.; Saunders, V. R. *J. Chem. Phys*. **1994**, *100*, 2128.

(3) Nelmes, R. J.; Loveday, J. S.; Wilson, R. M.; Besson, J. M.; Pruzan, Ph.; Klotz, S.; Hamel, G.;. Hull, S. *Phys. Rev. Lett.* **1993**, *71*, 1192.

(4) Besson, J. M.; Pruzan, Ph.; Klotz, S.; Hamel, G.; Silvi, B.; Nelmes, R. J.; Loveday, J. S.; Wilson, R. M.; Hull, S. *Phys. Rev. B* **1994,** *49*, 12540.

(5) The structural parameters of ice VIII have been determined recently by neutron diffraction up to 25 GPa. Besson, J. M.; Klotz, S.; Hamel, G.; Nelmes, R. J.; Loveday, J. S.; Marshall, W. G. To be published.

(6) Silvi, B. *Phys. Rev. Lett.* **1994**, *73*, 842.

(7) Benoit, M.; Bernasconi, M.; Focher, P.; Parrinello, M. *Phys. Rev. Lett.* **1996**, *76*, 2934.

(8) Pruzan, Ph; Chervin, J. C.; Canny, B. *J. Chem.Phys.* **1993**, *99*, 9842.

(9) Aoki, K.;Yamanaki, H.; Sakashita, M. *Phys. Rev. Lett.* **1996**, *76*, 784.

(10) Goncharov, A. F.; Struzhkin, V. V.; Somayazulu, M. S.; Hemley, R .J.; Mao, H. K. *Science* **1996**, *273*, 218.

(11) Holzapfel, W. *J. Chem. Phys.* **1972**, *56*, 712.

(12) Le Toullec, R.; Pinceaux, J. P.; Loubeyre, P. *High Pressure Research* **1988**, *1*, 77.

(13) Chervin, J. C.; Canny, B.; Gauthier, M.; Pruzan, Ph. *Rev. Sci. Instrum.* **1993**, *64*, 203.

(14) Wolanin, E.; Pruzan, Ph.; Chervin, J. C.; Canny, B.; Gauthier, M.; Häusermann, D.; Hanfland, M., *Phys. Rev. B.* Submitted for publication.

(15) Kuhs, M. F.; Finney, J. L.; Vettier, C.; Bliss, D. V. *J. Chem. Phys.* **1984**, *81*, 3612.

(16) Pruzan, Ph.; Chervin, J. C.; Gauthier, M. *Europhys. Lett.* **1990**, *13*, 8.

(17) Pruzan, Ph.; Chervin, J. C.; Canny, B. *J. Chem .Phys.* **1992**, *97*, 718.

(18) Wong, P. T. T.; Whalley, E. *J. Chem. Phys.* **1976**, *64*, 2359.

(19) Pruzan, Ph. *J. Mol. Struct.* **1994**, *322*, 279.

(20) Sherman, W. F. *J. Phys. C* **1982**, *15*, 9.

(21) Samara G.; Peercy, P. S. *Solid State Phys.* **1981,** *36*, 1.

(22) Pruzan, Ph.; Chervin, J. C.;Canny, B. *Proceedings of the XIVth International Conference on Raman Spectroscopy*; Yu, N. T., Li, X. Y. Eds.; John Wiley: New York, 1994; p 1048.

(23) Vinet, P.; Smith, J. R.; Ferrante, J.; Rose, J. H. *Phys. Rev. B* **1987**, *35*, 1945.

(24) Hemley, R. J.; Jephcoat, A. P; Mao, H. K ; Zha, C. S.; Finger, L. W.; Cox, D. E. *Nature* **1987**, *330*, 737.

(25) Novak, A. *Struct. Bonding (Berlin)* **1974**, *18*, 177.

(26) Olovsson, I.; Jönsson, P. G. In *The Hydrogen Bond II. Structure and Spectroscopy*; Schuster, P., Zundel, G., Sandorfy, C., Eds.; North-Holland: Amsterdam, 1976; p 393.

(27) Ichikawa, M. *Acta Crystallogr., Sect. B* **1978**, *34*, 2074.

(28) Schweizer, K. S.; Stillinger, F. H. *J. Chem. Phys.* **1984**, *80*, 1230.

(29) For example, see: Eckert, J.; Fincher, C. R.; Goldstone, J. A.; Press, W. *J. Chem. Phys.* **1981**, *75*, 3012.